Effects of counting rate and resolution time on a measurement of the intensity correlation function

Y. Li, G. Li, Y. C. Zhang, X. Y. Wang, J. Zhang, J. M. Wang, and T. C. Zhang*

State Key Laboratory of Quantum Optics and Quantum Optics Devices, Institute of Opto-Electronics, Shanxi University, Taiyuan 030006, China

(Received 4 February 2007; revised manuscript received 22 March 2007; published 25 July 2007)

Non-photon-number-resolving single-photon-counting modules (SPCM's), also called on-off photon detectors, have been used in quantum optics for investigating the properties of various light fields based on the Hanbury-Brown-Twiss (HBT) experiment. However, for different incident light fields the experimental conditions can affect the measured photon statistics. In this paper, the second-order degree of coherence $g^{(2)}$, known as the important factor for quantitying a single-photon source, is experimentally investigated by means of the HBT scheme consisting of two SPCM's. By comparing the results of coherent field with that of the thermal field, we show that the measured $g^{(2)}$ is affected by the photon-counting rate and the resolution time from pulsed to continuous wave fields. The proper counting rate and resolution time for characterizing the exact photon statistical properties of input fields are determined.

DOI: 10.1103/PhysRevA.76.013829 PACS number(s): 42.50.Ar

Photon-counting detection has been used to determine the photon statistical properties of light fields since the first experiment on intensity correlation [the Hanbury-Brown-Twiss (HBT) experiment] in 1956 [1]. Recently, the fast development of digitized single-photon-detection techniques has enabled us to investigate the nonclassical properties of light fields, such as quantum high-order correlations [2], photon antibunching effects [3], and single-photon sources (SPS's) [4] which play a very important role in quantum optics and quantum-information processing [5] for quantum computation, cryptology, and communication. A single-photon-counting module (SPCM) is an on-off non-photon-number-resolving detector. Each SPCM is a digitized module which consists of a silicon avalanche photodiode (APD) operated in the Geiger mode and an electronic amplifier to amplify and shape the pulse generated by the photons. The reverse-bias voltage across the APD exceeds the breakdown voltage and leads to the response for incident single photons. The Geiger-mode APD does not produce a linear current, but a current pulse [6]. The term "module" refers to a detector that is packaged and mounted on a case which contains the regulated power supply, active quench circuit, thermoelectric cooler, and output circuitry. Compared with photomultiplier tubes, SPCM's have high quantum efficiency, large wavelength coverage, and fast speed of response [6]. HBT experiments based on such SPCM's have become an important system to measure the nonclassicalities of light fields and to evaluate the quality of SPS's [4,7]. They are also used in various fields to investigate the statistical properties of photon emission, such as light scattering [8], cold atom physics [9], and quantum optics [10], etc.

The second-order degree of coherence $g^{(2)}$ can be directly determined via single SPCM's [11], but the dead time of the SPCM limits the resolution time, and a single SPCM also limits the effective dynamic range of the incident light intensity. Although photon-number-resolving detectors [12,13] are able to resolve the arrived photon number, they are still being developed and have not been commercialized. Two or more SPCM's are still the best choice to measure the high-order correlation of light fields at the present time. Compared to single SPCM's, the main advantage with two or more SPCM's based on HBT schemes is that they can avoid the limitation of the dead time of detectors and can increase the intensity range. The measured photon properties of the different incident light fields can be profoundly affected by experimental conditions [7,14]. The actual nonideal measurement conditions and such on-off SPCM's themselves make it difficult to understand correctly and truly the original statistical properties of the incident light field. In this paper, the photon statistical properties of coherent and thermal fields are experimentally studied, from pulsed to continuous operation, by means of a HBT scheme consisting of two SPCM's operating in Geiger mode. The results show that, although the measured second-order degree of coherence is strongly affected by the photon-counting rate and resolution time, when the proper experimental conditions are chosen (here for example, about 50 kcounts/s for the counting rate and 32 ns for the resolution time), the results can reflect correctly the photon statistical properties of coherent and thermal fields. Our experimental results are confirmed by a theoretical analysis. The results reported here, for the first time to our knowledge, can provide some substantive information for photon statistical investigation to experimentalists, especially for the nonclassical properties of various quantum states of light fields, which are even more strongly affected by the detection process of these on-off SPCM's and experimental conditions [7].

Let us consider an incident pulsed coherent beam which is a series of rectangle shaped pulses. If the intensity of each pulse I_0 is constant, then the average intensity of the beam is $\bar{I}=fI_0$, where f is the ratio of the pulse width τ_0 to the period T_0.

The second-order degree of coherence is [15]

*Author to whom correspondence should be addressed. tczhang@sxu.edu.cn

$$g^{(2)}(\tau) = \frac{\langle \bar{I}(t)\bar{I}(t+\tau)\rangle}{\bar{I}^2}. \quad (1)$$

Here τ is the delay time. When τ equals zero, the zero-delay second-order degree of coherence is [15]

$$g^{(2)}(0) = \frac{1}{f}. \quad (2)$$

Otherwise, the second-order degree of coherence is the convolution of two periodic rectangle-shaped pulses. When $\tau_0 \leqslant T_0/2$,

$$g^{(2)}(\tau) = \begin{cases} \frac{\tau/T_0 + f - m}{f^2}, & mT_0 - \tau_0 \leqslant \tau \leqslant mT_0, \\ \frac{f - \tau/T_0 + m}{f^2}, & mT_0 \leqslant \tau \leqslant mT_0 + \tau_0, \\ 0, & mT_0 + \tau_0 \leqslant \tau \leqslant mT_0 + T_0 - \tau_0, \end{cases} \quad (3)$$

where m is an integer, and for $\tau_0 \geqslant T_0/2$

$$g^{(2)}(\tau) = \begin{cases} \frac{\tau/T_0 + f - m}{f^2}, & mT_0 - (T_0 - \tau_0) \leqslant \tau \leqslant mT_0, \\ \frac{f - \tau/T_0 + m}{f^2}, & mT_0 \leqslant \tau \leqslant mT_0 + (T_0 - \tau_0), \\ \frac{2f - 1}{f^2}, & mT_0 + (T_0 - \tau_0) \leqslant \tau \leqslant mT_0 + \tau_0. \end{cases} \quad (4)$$

Thus $g^{(2)}(\tau)$ given by Eqs. (2)–(4), is a series of triangle-shaped pulses, as shown in Fig. 1(a). Both the maxima and minima of the triangle-shaped pulses tend to 1 as f increases.

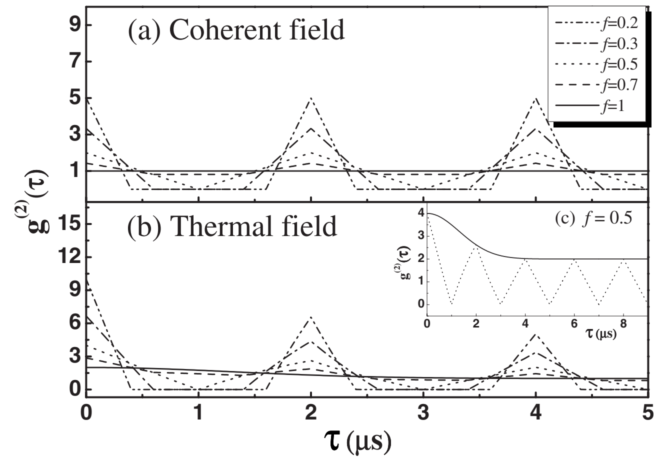

FIG. 1. $g^{(2)}(\tau)$ of pulsed coherent light (a) and thermal light with a Gaussian distribution for $\gamma = 0.000\,54\ \text{ns}^{-1}$ (b) versus the delay time for different f. f is the ratio of the pulse width τ_0 to period the T_0. The inset in (b) shows the result of a pulsed thermal light with Gaussian distribution ($f = 0.5$).

When $f = 1$, i.e., for a continuous wave, $g^{(2)}(\tau) = 1$. It shows that the maximum width of the triangle-shaped pulses of $g^{(2)}(\tau)$ of the coherent light is twice the width of the pulse.

The above results assume ideal light coherence with infinite coherent time. For a pulsed thermal light, with, e.g., a Gaussian distribution [1], the triangle-shaped pulses still remain, but they are modulated by a Gaussian function. The zero-delay second-order degree of coherence is

$$g^{(2)}(0) = \frac{2}{f}, \quad (5)$$

because of the bunching effect of the thermal light. In general, when $\tau_0 \leqslant T_0/2$,

$$g^{(2)}(\tau) = \begin{cases} \frac{\tau/T_0 + f - m}{f^2}[1 + \exp(-\gamma^2\tau^2)], & mT_0 - \tau_0 \leqslant \tau \leqslant mT_0, \\ \frac{f - \tau/T_0 + m}{f^2}[1 + \exp(-\gamma^2\tau^2)], & mT_0 \leqslant \tau \leqslant mT_0 + \tau_0, \\ 0, & mT_0 + \tau_0 \leqslant \tau \leqslant mT_0 + T_0 - \tau_0, \end{cases} \quad (6)$$

and when $\tau_0 \geqslant T_0/2$

$$g^{(2)}(\tau) = \begin{cases} \frac{\tau/T_0 + f - m}{f^2}[1 + \exp(-\gamma^2\tau^2)], & mT_0 - (T_0 - \tau_0) \leqslant \tau \leqslant mT_0, \\ \frac{f - \tau/T_0 + m}{f^2}[1 + \exp(-\gamma^2\tau^2)], & mT_0 \leqslant \tau \leqslant mT_0 + (T_0 - \tau_0), \\ \frac{2f - 1}{f^2}[1 + \exp(-\gamma^2\tau^2)], & mT_0 + (T_0 - \tau_0) \leqslant \tau \leqslant mT_0 + \tau_0. \end{cases} \quad (7)$$

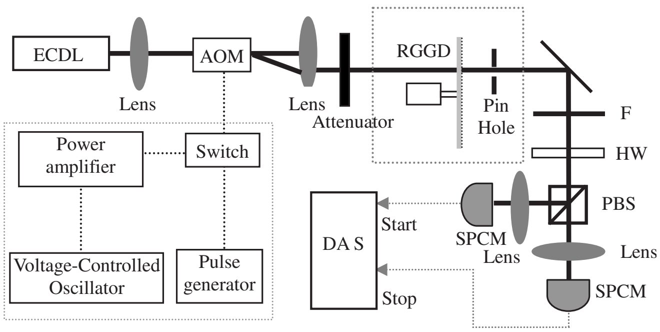

FIG. 2. Experimental setup. cw light from a diode laser (ECDL) at 905 nm is sliced into pulses using an acousto-optic modulator (AOM) driven by a pulse-controlling system (dashed line at the left). These pulses are filtered (F) and divided into two equivalent parts by a half-wave plate ($\lambda/2$) and polarization beam splitter (PBS). They are received by two SPCM's, respectively. The outputs of the SPCM's are sent into the data acquisition system (DAS).

Here $\gamma=1/\tau_c$, and τ_c is the coherence time of the thermal field. Figure 1(b) shows the results from Eqs. (5)–(7).

Figure 2 is the setup of the experiment. In our system, the laser pulses are generated from a cw home-made extended cavity diode laser (ECDL) by using an acousto-optic modulator (AOM, 3080-122, Crystal Technology, Inc.), which is driven by a rf signal at 80 MHz. The center wavelength is 905 nm. Two lenses are used to improve the diffractive efficiency of the first-order beam and collimate it.

The left dashed frame in Fig. 2 is the pulse-controlling system. In the experiment, the period of the light pulses is fixed at 2000 ns, corresponding to a 500 kHz repetition rate. The value of f can be changed by varying the pulse width.

Pulsed thermal light is produced by sending an attenuated and focused laser pulse beam onto a rotating ground glass disk (RGGD), which produces a pseudothermal field [1,16–18] (see the right dashed frame in Fig. 2). The beam goes through a pinhole and a filter (F) and is divided into two equal parts by a half-wave plate ($\lambda/2$) and a polarization beam splitter (PBS). The transmitted and reflected beams are focused on two single-photon-counting modules (SPCM-AQR-15, PerkinElmer Optoelectronics). The quantum efficiency of the module given by the manufacturer is about 35% at 900 nm and the dark count of the module is less than 55 counts/s. The output pulses of the two SPCM's enter the start and stop channels of the data acquisition system (DAS, P7888, Fastcomtec, GmbH), respectively. The coincidences of the two channels can be obtained and the second-order degree of coherence $g^{(2)}(\tau)$ of the incident light field can be determined after the data normalization.

Figure 3 shows the second-order degree of coherence of the coherent light and thermal light versus the delay time τ with different pulse widths and fixed period (2000 ns). The counting rate of each measurement remains 50 kcounts/s and the resolution time is 32 ns. (We show only the data for $\tau>0$; the results for $\tau<0$ are just mirror symmetric.) The results in Figs. 3(a)–3(d) correspond to 600, 1000, and 1400 ns pulse widths and a continuous wave, respectively. Here, the black crosses are the measured results of the thermal light while the gray dots are the results for coherent light. The black lines in Figs. 3(a)–3(d) correspond to the theoretical results for pulsed thermal light given by Eqs. (5)–(7). Here $\gamma=0.000\,54$ ns^{-1}. The gray lines are the theoretical results for coherent light based on the relations of Eqs. (2)–(4).

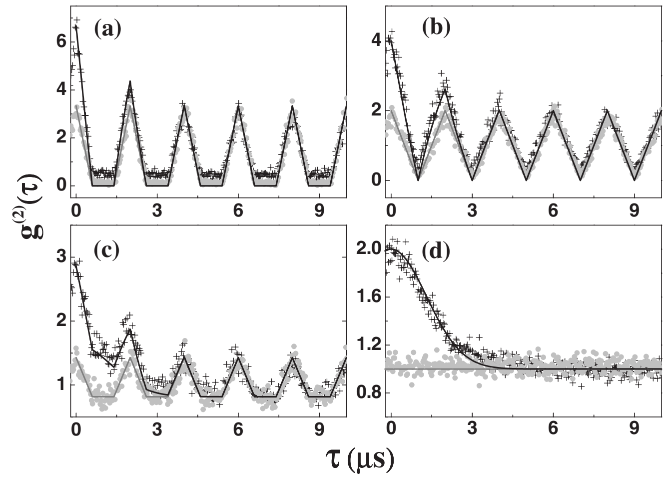

FIG. 3. $g^{(2)}(\tau)$ of coherent and thermal light versus the delay time τ with different f. The counting rate is 50 kcounts/s and the resolution time is 32 ns. From (a) to (d), f equals 0.3, 0.5, 0.7, and 1, respectively. The black crosses and gray dots are the experimental results of pulsed thermal light and coherent light, respectively. The black lines and the gray lines refer to their theoretical results. For the theoretical results of the thermal light with a Gaussian distribution, the parameter γ equals 0.000 54 ns^{-1}.

Clearly, the statistical behaviors of the coherent field and thermal field are very distinguishable. The measured $g^{(2)}(\tau)$ of the coherent light oscillates periodically with equal amplitudes, while for the thermal light, it shows a damping oscillation and the maximum value appears at $\tau=0$. The result for the continuous wave satisfy a Gaussian distribution. The experimental results for coherent and thermal light are in accordance with the theoretical analysis. The minor discrepancy between theory and experiment for the thermal field at small delay time may be due to several factors. Clearly, the characteristic of the thermal distribution directly determines how fast $g^{(2)}(\tau)$ decreases as τ increases. We have chosen a Gaussian distribution [1] to fit the data but the real distribution may not be ideal Gaussian. The second factor is that the "thermal state" generated by rotating ground glass is not a pure thermal state, but certainly a mixture of a pure thermal state plus a coherent state, which directly affects the bunching properties. We do not know exactly how much pure thermal light is in the mixture (this is mainly determined by the scattering of the rotating ground glass and the background environment of the experiment), but the ratio of these two parts has a remarkable effect on the bunching [19].

If we fix the average counting rate of the pulsed light at 50 kcounts/s, and vary the ratio value f for each measurement, the results as shown in Fig. 4. (The symbols are the same as in Fig. 3.) From Fig. 4(a)–4(d), f equals 0.3, 0.5, 0.7, and 1, respectively, and the corresponding counting rate for each measurement is 167, 100, 70, and 50 kcounts/s, respectively. We can see that there exists a larger discrepancy

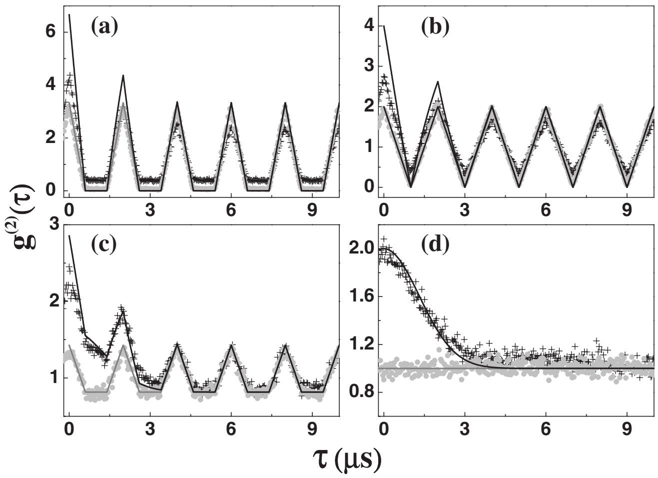

FIG. 4. $g^{(2)}(\tau)$ of coherent and thermal light versus the delay time τ with different f. The average counting rate is 50 kcounts/s and the resolution time is 32 ns. From (a) to (d), f equals 0.3, 0.5, 0.7, and 1, respectively. The symbols are the same as in Fig. 3.

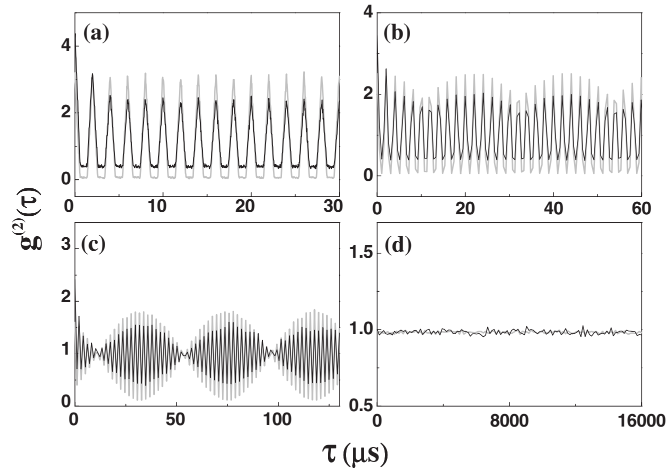

FIG. 5. $g^{(2)}(\tau)$ of coherent and thermal light versus the delay time when the counting rate is 50 kcounts/s, pulse width is 600 ns, and f=0.3, corresponding to the resolution time T (a) 2^5, (b) 2^9, (c) 2^{10}, and (d) 2^{17} ns. The black and gray lines are the experimental results for the thermal and coherent fields, respectively.

between the measured maxima of $g^{(2)}(\tau)$ and the theoretical analysis for the pulsed thermal light. A smaller f corresponds to a larger discrepancy, which shows that the counting rate affects the measured results. For a higher count rate, the incident photon number is higher and such a non-photon-number-resolving SPCM gets a higher photon-number-counting error [7].

We also investigate $g^{(2)}(\tau)$ as a function of the delay time for different resolution times. Figure 5 shows the results when the counting rate is 50 kcounts/s, and f=0.3 (τ_0 =600 ns). The black and gray lines are the experimental results for thermal and coherent fields, respectively. When the resolution time T increases from 2^5 to 2^{17} ns, the measured $g^{(2)}(\tau)$ for both coherent and thermal fields undergoes an initially regular oscillation, then modulated oscillation, and tends to unity eventually. This shows that the measured $g^{(2)}$ $\times(\tau)$ strongly depends on the resolution time T.

The above results can be reasonably understood as follows: basically, a longer resolution time T of the DAS implies a lower resolving ability for the signals. When the resolution time is short, the system can resolve the pulse sequences as expected [Fig. 5(a)]. When the resolution time gets longer and reaches the pulse width, the system cannot resolve each light pulse but selects part of each one to measure, and the total result shows a modulated oscillation [Figs. 5(b) and 5(c)]. When the resolution time far exceeds the pulse width, the system just randomly chooses the measurement point by point from the large number of pulses, which corresponds to a Poissonian distribution regardless of whether the light is coherent or thermal, and that implies that $g^{(2)}(\tau)$ is close to 1 for both coherent light and thermal light [Fig. 5(d)]. Actually, as the resolution time gets longer and longer, it tends to the case of a continuous wave. In order to characterize the real input light pulse, the resolution time should be much shorter than the width of the light pulse. Here the typical resolution time in the experiment is 32 ns.

In conclusion, the second-order degree of coherence of coherent and thermal light from pulsed to cw operation is experimentally studied and analyzed with on-off SPCM's. Both the experiment and analyses show that the second-order degree of coherence can be profoundly affected by the counting rate and the ratio of the pulse width to the period, f. To truly characterize the photon statistical properties of the incident light fields, the resolution time should be much shorter than the pulse width and the coherent time.

ACKNOWLEDGMENTS

This work was supported by NSF of China (Grants No. 10434080 and No. 60578018), the 973 program (Grant No. 2006CB921102), and also by the CFKSTIP and PCSIRT from the Ministry of Education of China.

[1] H. R. Brown and R. Q. Twiss, Nature (London) **177**, 27 (1956).
[2] F. T. Arecchi, A. Berné, and P. Bulamacchi, Phys. Rev. Lett. **16**, 32 (1966).
[3] H. J. Kimble, M. Dagenais, and L. Mandel, Phys. Rev. Lett. **39**, 691 (1977).
[4] J. McKeever, A. Boca, A. D. Boozer, J. R. Buck, and H. J. Kimble, Nature (London) **425**, 268 (2003).
[5] J. S. Neergaard-Nielsen, B. M. Nielsen, C. Hettich, K. Mølmer, and E. S. Polzik, Phys. Rev. Lett. **97**, 083604 (2006); D. N. Matsukevich, T. Chanelière, S. D. Jenkins, S.-Y. Lan, T. A. B. Kennedy, and A. Kuzmich, *ibid.* **97**, 013601 (2006).
[6] Carl Jackson, http://photondetection.com/pub/top
[7] G. Li, T. C. Zhang, Y. Li, and J. M. Wang, Phys. Rev. A **71**, 023807 (2005).
[8] J. K. Phalakornkul, A. P. Gast, R. Pecora, G. Nägele, A. Fer-

rante, B. Mandl-Steininger, and R. Klein, Phys. Rev. E **54**, 661 (1996).

[9] J. Volz, M. Weber, D. Schlenk, W. Rosenfeld, J. Vrana, K. Saucke, C. Kurtsiefer, and H. Weinfurter, Phys. Rev. Lett. **96**, 030404 (2006).

[10] K. J. Resch, G. G. Lapaire, J. S. Lundeen, J. E. Sipe, and A. M. Steinberg, Phys. Rev. A **69**, 063814 (2004).

[11] Y. Li, G. Li, Y. C. Zhang, X. Y. Wang, J. M. Wang, and T. C. Zhang, Acta Phys. Sin. **56**, 5779 (2006).

[12] D. Rosenberg, A. E. Lita, A. J. Miller, and S. W. Nam, Phys. Rev. A **71**, 061803 (2005).

[13] D. Achilles, C. Silberhorn, C. Sliwa, K. Banaszek, I. A. Walmsley, M. J. Fitch, B. C. Jacobs, T. B. Pittman, and J. D. Franson, J. Mod. Opt. **51**, 1499 (2004).

[14] F. Treussart, R. Alléaume, V. Le Floch, L. T. Xiao, J.-M. Courty, and J. F. Roch, Phys. Rev. Lett. **89**, 093601 (2002).

[15] R. Loudon, *The Quantum Theory of Light* (Advanced Education Press, Beijing, 1992).

[16] J. W. Goodman, *Statistical Optics* (Science Press, Beijing, 1992).

[17] L. Basano and P. Ottonello, Am. J. Phys. **50**, 996 (1982).

[18] W. Martienssen and E. Spiller, Am. J. Phys. **32**, 919 (1964).

[19] Gang Li, Tiancai Zhang, Tao Geng, Yuchi Zhang, and Junmin Wang, Proc. SPIE **5631**, 134 (2005).